Ion-track model for fast-ion-induced desorption of molecules

A. Hedin, P. Håkansson, and B. Sundqvist

Tandem Accelerator Laboratory, University of Uppsala, Box 533, S-751 21 Uppsala, Sweden

R. E. Johnson

Department of Nuclear Engineering and Engineering Physics, University of Virginia, Charlottesville, Virginia 22901

Recent data on the desorption of large biomolecules by fast (MeV) ions are examined with use of the ion-track model derived from "hit" theory commonly used in radiation biology. In this model, desorption requires that a given molecule be "hit" by m secondary electrons produced by the incident ion. Those molecules penetrated by the fast ion, and hence receiving large doses of radiation, will be damaged, whereas those receiving m "hits" at a distance from the track may be ejected as whole molecules with probability which varies from about 0.4% to 4% for the molecules considered. The model is shown to describe the nonlinear behavior at small values of dE/dX, the electronic energy loss per unit path length, giving way to a linear behavior (saturation) at large dE/dX. For the best fits to the available data at constant ion velocity, m increases with the size of the molecule and the survival probability tends to decrease with size, although the behavior of the latter quantity is much more susceptible to uncertainties in the model. Furthermore, the dependence of yield on velocity is well described over a broad range of ion velocities. These results suggest this model can be used to unify the data taken for a variety of targets, incident ions, and ion energies. Although the model does not give insight into the exact desorption mechanism, it strongly suggests that desorption is due to the breaking of bonds by the shower of secondary electrons generated by the passing ion.

INTRODUCTION

Mass spectrometry is a widely used tool for studying small biomolecules of interest in the biological sciences. Conventional mass-spectrometric methods have limitations, however, for large molecules. It is often difficult to produce undissociated, gas-phase ions of high-mass molecules, and the mass-analyzing magnets become very huge and thus expensive.

An attempt to solve this problem was made in 1974 (Ref. 1) when Macfarlane and co-workers suggested that fission fragments from a radioactive nucleus, ^{252}Cf, could be used to desorb and ionize biomolecules from a surface. These molecular ions were then mass-analyzed with a time-of-flight technique.[2] This new method has been particularly successful for heavy, nonvolatile, and thermally labile biomolecules. The first mass spectra of bovine insulin, MW 5733,[3] were obtained in this manner and later, even larger proteins, such as a neutrotoxin, MW 7821,[4] and a tiger-snake-venom component, MW 13309,[5] were studied.

In order to fully exploit this technique in future applications, a knowledge of the underlying desorption process is important. Furthermore, this process is of interest in itself, as the mechanism for desorption appears to be a new physical process not directly related to the well-known, low-energy sputtering of metals.[6] Rather, the desorption process discussed here appears to be similar to that occurring in many insulating materials,[7] and is related to the electronic stopping of the primary ion.[8]

In order to understand the desorption mechanism, monoenergetic ion-beam experiments have supplanted the fission-fragment methods. In these experiments, the primary ion parameters of velocity,[8] mass,[8] charge state,[9] angle of incidence,[10] and energy loss[11] are varied systematically. In the experiments to be analyzed here, an amino acid, two protected oligonucleotides, and insulin were irradiated with different ions, but at the same ion velocity (Table I). The data for these molecules indicated that the energy density required for desorption increased with the physical size of the molecule. It was also found that above a certain energy density the yield increased linearly with the deposited energy, in contrast to the behavior at low-energy densities, where the yield increases faster than linearly with energy density. Such a behavior is suggestive of ion-track models developed from "hit" theory.

In this paper we test the applicability of an ion-track model for the desorption process. The model considered here, as originally developed by Katz et al.,[12] has been used to describe bulk interactions where the detected event is caused by secondary electrons (δ rays) ejected from the ion track in the bombarded medium. Examples of applications are blackening of nuclear emulsions, inactivation of biological material such as viruses and enzymes, and the response of particle detectors such as scintillators.[12] Here, we apply the model to phenomena occurring close to a surface. We are confident that this is not a severe limitation, partly because desorption yields are roughly the same whether the sample is bombarded from the front or back, indicating that the secondary electrons can be treated as being essentially ejected perpendicular to the ion track. Furthermore, in collecting the experimental data analyzed in the model, charge equilibrium of the primary ions was established before the ions impinged on the sam-

TABLE I. Yield of full mass secondary ions as a percent of the number of primary ions.

Target	10.3	15.9	34.1	59.1	99.1
			dE/dX (MeV/mg cm^{-2})		
Valine	1.3	2.3	8.8	21.0	30.0
2-valine	0.23	0.48	2.4	6.2	9.3
3-valine	0.040	0.11	0.65	1.8	2.9
4-valine		0.040	0.24	0.59	0.91
AAC		0.090	0.86	1.7	2.6
CAACCA		0.017	0.26	0.43	0.73
Insulin$^+$		0.044	0.48	2.5	3.7
Insulin$^-$		0.010	0.24	1.0	2.4

ple by letting the beam pass through a thin gold foil. Although the data are too sparse to unambiguously determine all the parameters in the model, the trends in the yield variation with energy loss and target-molecule-size increases are those predicted by the model. This will hopefully serve to unify the data on diverse systems, and also as an inspiration to collect new data in a systematic way. Finally, we consider two other descriptions of the desorption process.

THE MODEL

Of the total amount of the energy deposited electronically in a target by a fast ion, $\approx 40\%$ is deposited as primary excitations and ionizations close to the ion's path, and the remaining $\approx 60\%$ is energy-deposited by secondary electrons produced as a result of the primary processes.[13] These two regions of energy deposition[14] are termed "infratracks" $(r = 1-10$ Å) and "ultratracks" $(r = 100-1000$ Å). The energy deposited by the secondary electrons at or near the target surface causes desorption of an ion via the rupture of a number of weak (hydrogen and van der Waals) bonds. Such bond ruptures may be directly produced by an electron traversing the surface or on the repulsive relaxation of an excitation produced close to the surface by the electron, as discussed by Johnson and Sundqvist.[15]

As the fast-ion—secondary-electron—induced desorption process requires the disruption of the binding of a biomolecule to its neighbors, the treatment given in the following is slightly different from the bulk damage models. It is assumed that a certain number of electrons, m, are required to hit a molecule (i.e., traverse the surface) to cause desorption. We are not concerned with the detailed mechanism of the desorption process at present, but only assume that it is caused by the electrons. Although the energy spread in the cloud of secondary electrons is large, the stopping power for electrons in biological material can be taken, to a good approximation, to be energy independent.[17] Therefore, the energy density deposited by the secondary electrons at a point in the target, which is a well-known quantity, is roughly proportional to the number of electrons that have passed through a unit area at that point. Knowing the electronic energy density deposited in the vicinity of a molecule, the average number of electrons that hit that molecule can be estimated. Writing ε_0 (eV/Å) as the stopping power of the electrons

in the target, then at a deposited-energy density e (eV/Å^3), there will be an average integrated fluence of e/ε_0 electrons per unit area (Å^2). If the molecular volume is written roughly as L^3, then $\lambda = L^2 e/\varepsilon_0$ is the average number of δ electrons hitting the molecule. Assuming the probability of a hit is Poisson distributed, then the probability of hitting a molecule X times is

$$p(X) = \frac{\lambda^X e^{-\lambda}}{X!} .$$

Hence the probability of at least m hits is

$$P(\geq m, \lambda) = \sum_{X=m}^{\infty} \frac{\lambda^X e^{-\lambda}}{X!} .$$

This is called the multiple-hit approach.[16] Assuming, instead, that m different targets on or close to the molecule must be hit at least once is the multiple-target approach,[16] discussed in the Appendix.

As the energy density is very nearly cylindrically symmetric with respect to the ion track, we write $e = e(r)$, r being the perpendicular distance to the track. The desorption cross section σ is found by integration over all r:

$$\sigma = \int_0^{\infty} 2\pi r P_s(r) P(\geq m, \lambda(r)) dr .$$

Here, $P_s(r)$, the survival probability, is the probability that the desorbed molecule is not destroyed by the energy deposited. This quantity is obviously very sensitive to molecular structure. Owing to the very high primary energy deposition in those molecules penetrated by the fast ion, we assume $P_s(r)$ to be 0 for $0 < r < r_d = L/2 + 1$ Å, where 1 Å is roughly the radius of the fast ion and L is the linear size of the molecule as before. A molecule with its center within a distance r_d from the ion path will be penetrated by the fast ion and thus be fragmented with unit efficiency by the primary energy. For $r > r_d$, $P_s(r)$ is assumed to be constant, P_s. The cross section, therefore, becomes

$$\sigma = p_s \int_{r_d}^{\infty} 2\pi r P(\geq m, \lambda(r)) dr . \tag{1}$$

As there have been large numbers of studies on the destruction of biomolecules by ionizing radiations,[14,16] $P_s(r)$ may be treated more accurately. We have also considered the case where $P_s(r)$ is a survival function which is determined by the Poisson distribution and the energy density deposited. This did not cause any significant difference in the results to be discussed.

The range-energy relation of electrons in biological material can be approximated as[17]

$$R = (0.991T)/\rho \text{ Å} ,$$

valid for electron energies, T (eV), up to 1 keV, where ρ is the density of the target in g/cm^3. Hence,

$$\varepsilon_0 = \rho/0.991 \text{ eV/Å} . \tag{2}$$

The deposited energy density $e(r)$ is estimated in the following way:

(a) For a given primary ion velocity, there is a maximum distance τ perpendicular to the track to which δ rays penetrate, the range of the most energetic electrons from the ion-electron collisions. This range, equal to the radius of the ultratrack, is proportional to the energy per amu (v^2) of the incoming particles,[17]

$$\tau = (3.9 \times 10^5/\rho)(v/c)^2 \text{ Å} .$$

A 1-MeV/amu ion gives a τ of ≈ 680 Å in valine $(\rho = 1.23)$.

(b) The radial dependence of e is approximated as $1/r^2$ for $r > 1$ Å. This is a consequence of the distribution of electron energies produced in close ion-electron collisions, and the near-linear range-energy relation of the electrons. More detailed distribution functions have been measured,[18] but this simple one is sufficient for the discussion.

(c) Furthermore, at the velocities of interest, approximately 60% of the energy deposited by the ions is lost to secondary electrons. As we are interested only in the energy deposited outside the track core, we assume in the following that about 50% of the total dE/dX is available as δ rays beyond $r = 1$ Å, so that

$$\int_{1\text{ Å}}^{\tau} 2\pi r e(r) dr \approx 0.5(dE/dX) .$$

Hence, we obtain, for $e(r)$,

$$e(r) = \begin{cases} \dfrac{0.5(dE/dX)}{2\pi(\ln\tau)r^2}, & 1 \text{ Å} < r < \tau \\[2mm] 0, & \tau < r < \infty. \end{cases} \tag{3a}$$

This is consistent with the results of Fain et al.[13] The expression describes the deposited energy density per unit length in the target. Typically, a 16-MeV ^{16}O ion incident on valine would, in this picture, deposit 2 eV/Å^3 at $r = 1$ Å, and, hence, 0.02 eV/Å^3 at $r = 10$ Å. The strength of a hydrogen bond is 0.1–0.3 eV and the bond length ≈ 1 Å, making the characteristic energy density required to break a hydrogen bond 0.1–1 eV/Å^3. The amount of energy deposited in the first monolayer (≈ 5 Å) of the valine target is ≈ 2 keV, and, hence, about 1 keV as secondary energy beyond $r = 1$ Å, which is sufficient to break large numbers of hydrogen and covalent bonds (0.1–0.3 and 2–4 eV/bond, respectively). The value of dE/dX are taken from the tables of Northcliffe and Shilling.[19] More accurate tables are available,[20] but they do not cover the entire energy range studied in our experiment.

Since $e(r)$ varies as r^{-2} from $r = 1$ Å, and L is typical-

ly 10 Å, considerable variations in energy density will occur within a molecule close to the ion track. Therefore we shall use the average energy density $\bar{e}(r)$,

$$\bar{e}(r) = (1/V_{\text{mol}}) \int_{V_{\text{mol}}} e(\mathbf{r}) dV ,$$

where V_{mol} is the volume of a molecule centered a distance r from the track. This is accomplished by replacing $1/r^2$ by

$$(1/2rL)\ln[(r+L/2)/(r-L/2)] ,$$

which is the analytical result obtained if one assumes the molecules located at r make up an annular shape about the track of extent L. More sophisticated averaging procedures have been used,[21] and ours are in good agreement with those. The averaging is important only close to the track. In Fig. 1, $\bar{e}(r)/e(r)$ is plotted versus r expressed in units of L. $e(r)$ thus becomes

$$e(r) = \frac{0.5(dE/dX)\ln[(r+L/2)/(r-L/2)]}{2\pi(\ln\tau)2rL} ,$$

$$1 \text{ Å} < r < \tau . \tag{3b}$$

We now replace λ by $\bar{\lambda}(r) = \bar{e}(r)L^2/\varepsilon_0$ in Eq. (1) and use Eqs. (2) and (3b) to obtain the final expression for the desorption cross section.

By way of understanding the dependence on m, σ plotted versus dE/dX for different values of m is shown in Fig. 2(a). For values of dE/dX fulfilling

$$\frac{L^2\bar{e}(r)}{\varepsilon_0} \ll 1 \text{ for } r > r_d ,$$

the integrand can be expanded to show that on the logarithmic plots the slopes of σ are approximately proportional to m in this region.

For values of dE/dX such that $L^2\bar{e}(r)/\varepsilon_0 > m$ in part of the δ-electron range, σ depends linearly on dE/dX independently of m. The saturation is a result of the r^{-2} dependence of e and, of course, at very high dE/dX the region of significant molecular damage will grow beyond r_d, that is, $P_s(r)$ will change. Varying L is seen in Fig. 2(b) to change the onset of the saturation. Hence, the
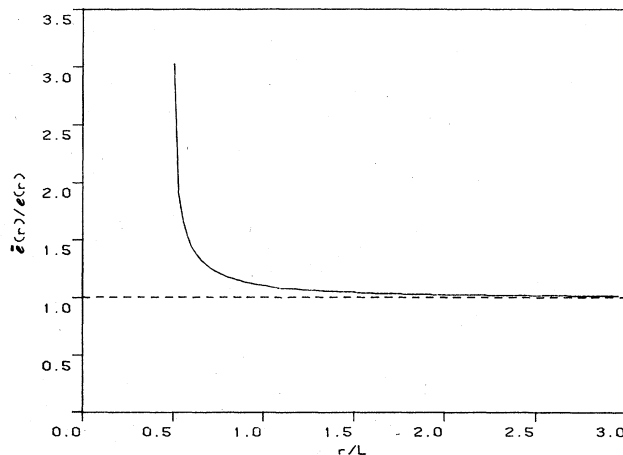
FIG. 1. $\bar{e}(r)/e(r)$ vs r/L. (Further explanations in text.)
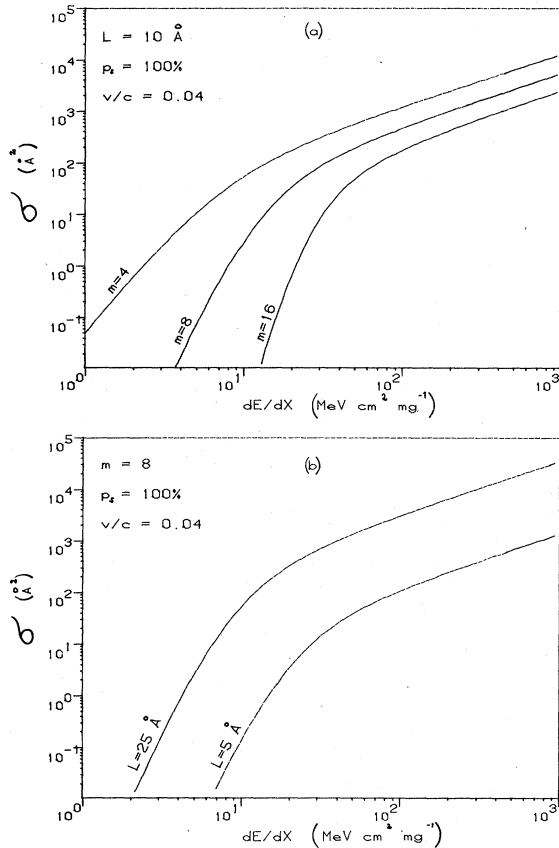
FIG. 2. (a) σ vs dE/dX for various m values. $L=10$ Å, $v/c=0.04$, and $\rho=1$. (b) σ vs dE/dX for various L values. $m=8$, $v/c=0.04$, and $\rho=1$.

ion-track model predicts the observed saturation effect at large dE/dX and a size effect at low dE/dX via m and L. Figure 3 shows the dependence of Y on v/c for different values of m. This has been a standard format for presenting desorption data on these systems, but the
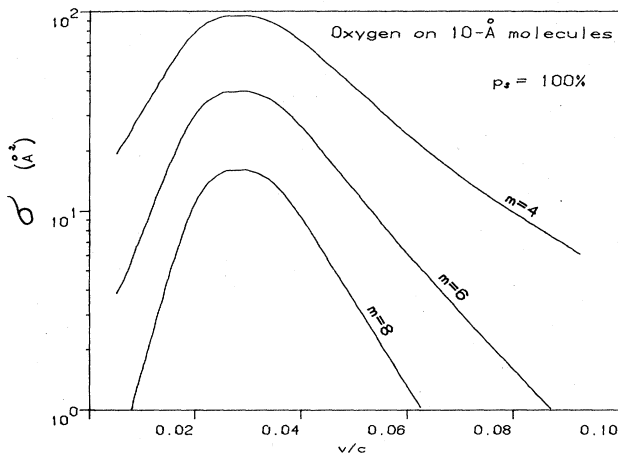
FIG. 3. σ vs v/c for various m values. dE/dX values of ^{16}O incident on biological material. $L=10$ Å, $v/c=0.04$, and $\rho=1$.
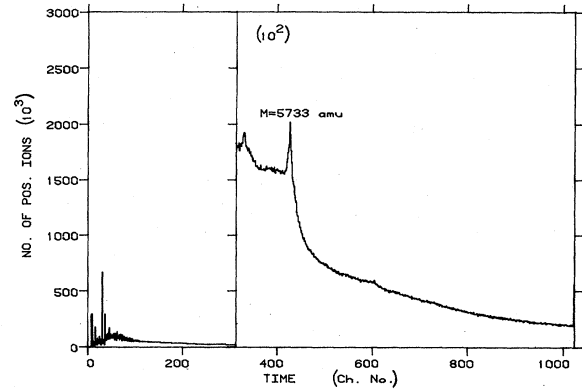
FIG. 4. Spectrum of bovine insulin, positive ions. The region to the left of the insulin peak is dominated by fragments.

saturation effect is obscured in such plots.

The yield Y (%) is expressed as the number of detected molecular ions per incident ion. In order to obtain Y from the desorption cross section, we write

$$Y \approx \lambda_s n_M \sigma ,$$ (4)

where n_M is the molecular-surface number density, L^{-2}, and λ_s is the number of layers ejected by the incident ion. Experiment indicates[22] that only a small fraction of the ejected-ion yield is desorbed as whole molecular ions and that the yield is predominantly fragments; see Fig. 4. In the following we presume the whole ions exit from the first layer, $\lambda_s=1$, and, as before, that they are ejected beyond a distance r_d from the track. Hence, $(\lambda_s n_M)^{-1}$ in the following is the geometric surface area of the molecules in the sample, L^2; that is, at least as far as whole ions are concerned, this is a desorption experiment. This is probably a very reasonable assumption for the large molecules. Based on the total mass ejected per incident ion in the sputtering of water ice[23] (a hydrogen-bonded material), the net number of equivalent large molecules ejected per incident ion is small. (It is clear that the total material loss per ion incident should be monitored in such experiments.) On the other hand, for the heavier ions on valine one would expect *more* than a monolayer to be desorbed. When more than a monolayer is removed, ejection of molecules from lower layers depends on the ejection from upper layers, and, hence, the details of the ejection process must be known. Again, based on the sputtering experiments,[7,23] a large fraction of the net ejecta is probably neutral. It is important to note that all the above uncertainties, together with the detection effeciency of the spectrometer, which is mass dependent and ranges from 20—80 %, will essentially affect the determination of p_s in our model.

EXPERIMENT VERSUS THEORY

The model has been fitted to experimental results of yield versus energy loss, dE/dX, and yield versus ion velocity for various systems. As mentioned earlier, the ion velocity was kept constant ($v/c=0.04$), in the

energy-loss experiments. This means that the inner and outer radii of the track are fixed so that only the energy density in the track, i.e., the number of electron hits per target molecule, varies.[11,22] The targets used in the energy-loss experiments were the amino acid valine, two protected oligonucleotides (AAC and CAACCA), and the proteins bovine insulin and phospholipase A_2 (P_β). In the case of insulin, the yields of both positive and negative ions were measured. It was not possible to obtain enough data points of P_β to make a meaningful fit. All molecule dimensions were estimated from molecule weights and target densities, $L = (M_{mol}/\rho)^{1/3}$. This simple approximation is adequate for our purpose. It should also be remembered that the molecules are, to some extent, randomly oriented on the surface, so that an average of L over a distribution of orientations should be used with the actual molecule structure. In fact, if a molecule is elongated, desorption as a whole molecule may occur more favorably for certain orientations.

In applying the model to the energy-loss experiments,[11] Table I, we plot $Y/(dE/dX)$ versus dE/dX to stress the saturation effect discussed earlier. The results are shown
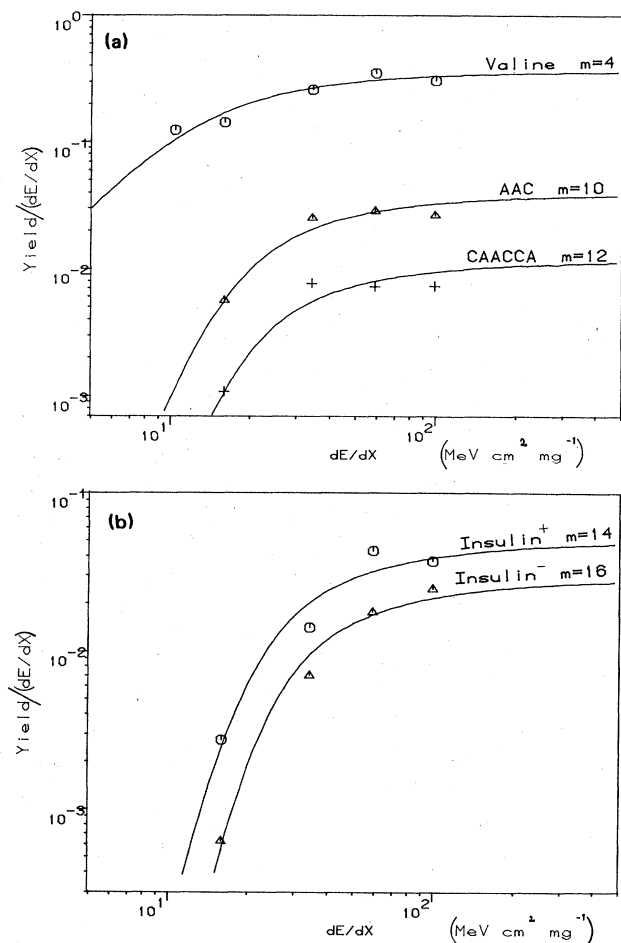
TABLE II. Data of fits in Figs. 5(a) and 5(b).

Target	Mass (amu)	L (Å)	m	m/L^2 (Å^{-2})	p_s (%)
Valine	117	5.4	4	0.14	2.8
AAC	1884	12.3	10	0.066	1.2
CAACCA	3609	15.2	12	0.052	0.31
Insulin$^+$	5734	19.4	14	0.037	1.6
Insulin$^-$	5733	19.4	16	0.043	1.1

in Figs. 5(a) (valine, AAC, CAACCA) and 5(b) (insulin) and Table II. We have used a least-squares fit to obtain the best values of m and p_s, where we have constrained m to be an integer. As can be seen in the figures, evidence of the two main predictions of the ion-track model, the saturation and size effects, are observed in the experiments. Although the data are sparse, the trends observed appear consistent with the model. Because both L and m have a role in the determination of the threshold behavior, more data, at lower dE/dX, are needed for most of the systems to verify the power-law dependence in the threshold region.

We have also fitted yield data of valine clusters given in Table I up to the tetramer, assuming that L is $5.4n^{1/3}$ Å, where n is the number of valine molecules in the cluster and 5.4 Å is L_{valine}. Again, the best values of p_s and m were obtained via a least-squares fit, and results are shown in Fig. 6 and Table III. Here, again, m is seen to increase with molecular size. However, since clusters are held together by weak forces, a clear decrease in p_s is also observed.

In Figs. 7(a) and 7(b), giving Y versus v/c, we have been able to fit data[24] of oxygen and sulfur incident on valine with the same m values. The observation of a fourth power in the dependence on dE/dX has been discussed elsewhere.[8] In general, however, those fits were not very good in the full velocity range measured. Using the present model, $Y \propto (dE/dX)^4$ at small dE/dX, but Y has a more complex dependence at other values. However, in

FIG. 5. (a) $Y/(dE/dX)$ vs dE/dX for valine, AAC, and CAACCA. See Table II. (b) $Y/(dE/dX)$ vs dE/dX for insulin$^+$ (positive ions) and insulin$^-$ (negative ions). See Table II.
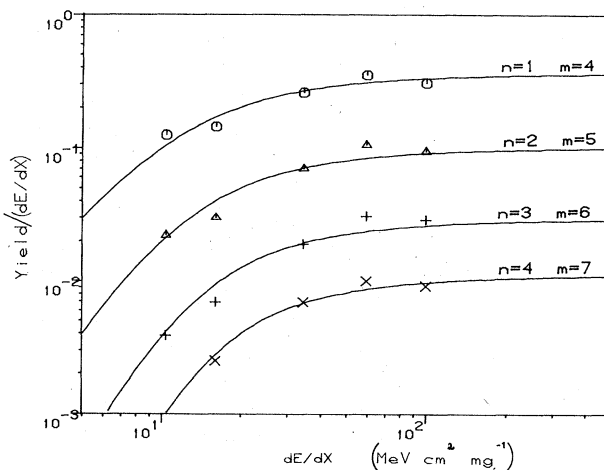
FIG. 6. $Y/(dE/dX)$ vs dE/dX for valine clusters. See Table III.

TABLE III. Data of valine cluster fits. See Fig. 6.

n	Mass (amu)	L (Å)	m	m/L^2 (Å^{-2})	p_s (%)
1	117	5.4	4	0.14	2.8
2	232	6.8	5	0.11	1.0
3	348	7.8	6	0.099	0.37
4	464	8.6	7	0.095	0.17

the fits shown in Fig. 7, the p_s shifted from the value of 2.8% (Table II) to 2.6% for oxygen, which is consistent, and to 1.1% for sulfur, which is not consistent. This uncertainty in p_s is most likely connected with our difficulty in knowing λ_m, our simplified treatment of $P_s(r)$, and the fact that the two experiments were carried out on different spectrometers.

OTHER MODELS

Recently, it has been suggested[25] that K-electron ionization in the target might be important for track formation and desorption. We have, for some of the cases mentioned above, used the cross section for these ionizations instead of dE/dX within the present "hit" model. The resulting velocity profile of σ_K generally shows less agreement with measured yields than the profile obtained using dE/dX. We further note that most of the inner-shell processes will occur within a distance r_d from the ion path, where we presume the survival probability is low. Those K-shell ionizations produced by δ rays are essentially included in our analysis via the energy deposition.

A number of authors have proposed thermal models for the desorption process.[26,27] In such a model the means of conversion of electronic energy into heat is not specified. In principle, however, a repulsive energy input in the track core region could dissipate via a thermal diffusion process. If the temperature in the vicinity of an undamaged surface molecule is sufficiently high to dissociate the weak bonds and persists long enough, then the residual expansion forces (e.g., Coulomb repulsion[28]) could eject molecules. Therefore, the yield should be determined by the average transient temperature increase, $\overline{T}(r)$, at a distance r from the ion's path, and the length of time, Δt, that this increase persists. Assuming the weight factor is the Maxwell-Boltzmann form, then

$$Y \propto \int_{r_d}^{\infty} \Delta t \exp(-U/k\overline{T})2\pi r \, dr \ ,$$

where U is the net bonding energy of the molecule to the surface (i.e., the sum of the weak bonds). Such an expression can be derived from first principles;[29,30] here we give it as a sensible result. Heat conduction in the materials of interest is complicated, but the results are generally not very sensitive to the details of the model.[30] We note that the form $\exp(-U/k\overline{T})$ can be written $[\exp(-U_0/k\overline{T})]^m$ if there are m bonds, each of binding energy U_0, holding the molecule to the surface. Therefore, this model has some similarities to the multiple-target model (see the Appendix). However, at large dE/dX it has been shown[29,30] that the yield saturates as $Y \propto (dE/dX)^2$ independent of the choice of the thermal model, and not linearly as observed in the experiments. This is a result of the time factor in the calculation of Y; that is, not only does the size of the spike grow as dE/dX increases, but it persists longer. Therefore a principal feature of the experiments cannot be described by the thermal model in its standard form. Finally, the energy densities deposited come into the yield expression (via $k\overline{T}$) in a way that is very different from the track models discussed here, implying that the threshold behavior predicted will also be very different.

FIG. 7. (a) Yield of valine when bombarded with [16]O at varying energy. (b) Yield of valine when bombarded with [32]S at varying energy. Data taken from Ref. 24.

CONCLUSIONS

The ion-track model used by Katz and co-workers to describe bulk radiation damage has been modified here to analyze desorption data for large biological molecules which are attached to each other by a number of hydrogen and van der Waals bonds. It is seen that such a model can be used to fit the data available rather well, describing both the nonlinearity in the yield at low dE/dX and the resulting linear behavior (saturation) at high dE/dX. The key to the validity of the model is whether or not the parameters obtained (m and p_s) are physically meaningful,

and whether or not a more reasonable choice of λ can be made which might yield very different values for these parameters. Here we have made the simple assumption that the desorbed molecule must be struck by a number of electrons. As we chose the energy-loss rate to be a constant, this implies that each electron is equally likely to disrupt (directly or indirectly[15]) the same number of bonds near the surface. It is therefore the effect of the shower of the secondary electrons which produces desorption in this model. Because this shower of electrons also disrupts internal bonds, desorbing a whole molecule is highly unlikely even if the requisite number of hits occurs; hence p_s is found to be small. p_s will be very sensitive to the molecular species (viz., Table II). However, the expected trend is seen, i.e., p_s decreases as the ratio of volume to surface area (i.e., L) grows. A larger variety of molecules of varying sizes, but with similar internal structure, should be examined. Beyond this, it is seen that it is easier to remove insulin$^+$ than insulin$^-$, as m is smaller for the former. (It may be a coincidence that both m and the net charge differ by two for these molecules.) One also expects that, as the size of the molecule increases, the number of hits must increase. This is seen to be the case in Tables II and III. Surprisingly, m is more nearly proportional to the molecular dimension L than to the surface area (L^2). However, at large m the value for m obtained in the fitting procedure is very sensitive to the choice of L, and, therefore, many more data points are needed in the threshold region. Furthermore, the model needs to be examined in terms of other values of the velocity for each species. The parameter m should be independent of velocity, as it is for valine (Fig. 7). In any case, a more detailed treatment of $P_s(r)$ and knowledge of the net amount of material removed are desirable.

APPENDIX: THE MULTIPLE-TARGET APPROACH

Instead of assuming that a molecule has to be hit m times by the secondary electrons (δ rays), one may assume that m specified targets must be hit, each at least once. The probability factor then becomes

$$[P(\geq 1, \bar{\lambda}(r))]^m = \{1 - \exp[-\bar{e}(r)l^2/e_0]\}^m ,$$

where l^2 is the cross section for the specified events. We have tried this approach as well and the fits are almost as good as in the multiple-hit case. However, assuming that the events driving the molecules from the surface are repulsive displacements resulting from excitations or ionizations,[15] then there are numerous locations near the surface at which such events can occur in a target molecule rather than m well-defined targets. This is our prime reason for choosing the multiple-hit approach. Clearly, as more data become available, the binding of the molecules to each other should be considered in more detail.

[1]D. F. Torgerson, R. P. Skowronski, and R. D. Macfarlane, Biochem. Biophys. Res. Commun. **60**, 616 (1974).

[2]R. D. Macfarlane and D. F. Torgerson, Int. J. Mass Spectrom. Ion. Phys. **21**, 81 (1976).

[3]P. Håkansson, I. Kamensky, B. Sundqvist, J. Fohlman, P. Peterson, C. J. McNeal, and R. D. Macfarlane, J. Am. Chem. Soc. **104**, 2948 (1982).

[4]P. Håkansson, I. Kamensky, J. Kjellberg, B. Sundqvist, J. Fohlman, and P. Peterson, Biochem. Biophys. Res. Commun. **110**, 519 (1983).

[5]I. Kamensky, P. Håkansson, J. Kjellberg, B. Sundqvist, J. Fohlman, and P. Peterson, FEBS Lett. **155**, 113 (1983).

[6]P. Sigmund, Phys. Rev. **184**, 383 (1969).

[7]R. W. Ollerhead, J. Böttiger, J. A. Davies, J. l'Ecuyer, H. K. Haugen, and N. Matsunami, Radiat. Eff. **49**, 203 (1980); F. Besenbacher, J. Bøttiger, O. Graversen, J. L. Hansen, and H. Sørensen, Nucl. Instrum. Methods **191**, 221 (1981); J. E. Griffith, R. A. Weller, L. E. Seiberling, and T. A. Tombrello, Radiat. Eff. **51**, 223 (1980); W. L. Brown, W. M. Augustyniak, E. Brody, B. Cooper, L. J. Lanzerotti, A. Ramirez, R. Evatt, and R. E. Johnson, Nucl. Instrum. Methods **170**, 321 (1980).

[8]P. Håkansson and B. Sundqvist, Radiat. Eff. **61**, 179 (1982).

[9]P. Håkansson, E. Jayasinghe, A. Johansson, I. Kamensky, and B. Sundqvist, Phys. Rev. Lett. **47**, 1227 (1981).

[10]P. Håkansson, I. Kamensky, and B. Sundqvist, Surf. Sci. **116**, 302 (1982).

[11]P. Håkansson, I. Kamensky, M. Salehpour, B. Sundqvist, and S. Widdiyasekera, Radiat. Eff. **80**, 141 (1984).

[12]R. Katz, Nuclear Track Detection 2, 1 (1978).

[13]J. Fain, M. Monnin, and M. Montret, Radiat. Res. **57**, 379 (1974).

[14]W. Brandt and R. H. Ritchie, in *Physical Mechanisms in Radiation Biology*, edited by R. D. Cooper and R. W. Wood (USAEC Technical Information Center, Oak Ridge, Tennessee, 1974), p. 20.

[15]R. E. Johnson and B. Sundqvist, Int. J. Mass Spectrom. Ion. Phys. **53**, 337 (1983).

[16]See, for example, H. Dertinger and H. Jung, *Molecular Radiation Biology* (Springer, New York, 1970), Chap. 2.

[17]E. J. Kobetich and R. Katz, Phys. Rev. **170**, 391 (1968).

[18]R. Katz, B. Ackerson, M. Homayoonfar, and S. C. Sharma, Radiat. Res. **47**, 402 (1971).

[19]L. C. Northcliffe and R. F. Shilling, Nucl. Data Tables 7, 233 (1970).

[20]J. F. Ziegler, *Stopping Cross-Sections For Energetic Ions In All Elements* (Pergamon, New York, 1980).

[21]R. Katz and E. J. Kobetich, Phys. Rev. **186**, 344 (1969).

[22]B. Sundqvist, A. Hedin, P. Håkansson, I. Kamensky, J.

Kjellberg, M. Salehpour, G. Säve, and S. Widdiyasekera, Int. J. Mass Spectrom. Ion. Phys. **53**, 167 (1983).

[23]W. L. Brown, L. J. Lanzerotti, and R. E. Johnson, Science **218**, 525 (1982); L. E. Seiberling, C. K. Meins, B. H. Cooper, J. E. Griffith, M. H. Mendehall, and T. A. Tombrello, Nucl. Instrum. Methods **198**, 71 (1982).

[24]A. Albers, K. Wien, P. Dück, W. Treu, and H. Voit, Nucl. Instrum. Methods **198**, 69 (1982); P. Dück, W. Treu, H. Fröhlich, W. Galster, and H. Voit, Surf. Sci. **95**, 603 (1980).

[25]T. A. Tombrello, Nucl. Instrum. Methods **230**, 555 (1984).

[26]R. D. Macfarlane and D. F. Torgerson, Phys. Rev. Lett. **36**, 486 (1976).

[27]R. W. Ollerhead, J. Böttiger, J. A. Davies, J. l'Ecuyer, H. K. Haugen, and N. Matsunami, Radiat. Eff. **49**, 203 (1980).

[28]P. K. Haff, Appl. Phys. Lett. **29**, 473 (1976); R. E. Johnson and W. L. Brown, Nucl. Instrum. Methods **198**, 103 (1982); C. C. Watson and T. A. Tombrello (unpublished).

[29]G. H. Vineyard, Radiat. Eff. **29**, 245 (1976).

[30]R. E. Johnson and R. Evatt, Radiat. Eff. **52**, 187 (1980).